Supporting Information

Ligand Substitution and Conformational Effects on the Ultrafast Luminescent Decay of $[Re(CO)_3(phen)(L)]^+$ (L=imidazole, pyridine): Nonadiabatic Quantum Dynamics

Maria Fumanal, Etienne Gindensperger, and Chantal Daniel

Laboratoire de Chimie Quantique Institut de Chimie de Strasbourg UMR 7177 CNRS-Université de Strasbourg 4 Rue Blaise Pascal, 67000 Strasbourg (France)

Section S1.

The intrastate, $\kappa^{(n)}$, and interstate, $\lambda^{(n,m)}$ coupling constants, where n and m label the electronic states, are extracted from the gradients and Hessians of the excited states, respectively, here evaluated at the Franck-Condon point (FC, $Q_i = 0$) and correspond to the following expressions, where V_n is the adiabatic potential energy surface of the state n obtained from quantum chemistry calculations.

For C_s symmetry with a' and a'' modes, it comes:

$$\kappa_i^{(n)} = \left.\frac{\partial V_n}{\partial Q_i}\right|_0 \quad \text{for } i \in \text{a'}$$

$$\lambda_i^{(n,m)} = \left.\left(\frac{1}{8}\frac{\partial^2}{\partial Q_i^2}\left(|V_m - V_n|^2\right)\right)^{1/2}\right|_0, \; n \neq m.$$

The later equation gives:

$$\lambda_i^{(n,m)} = \left.\left(\frac{\varepsilon_m - \varepsilon_n}{4}\left(\frac{\partial^2}{\partial Q_i^2} V_m - \frac{\partial^2}{\partial Q_i^2} V_n\right)\right)^{1/2}\right|_0$$

for $i \in$ a" and states n and m of different spatial symmetry and for $i \in$ a' and n and m of same spatial symmetry, with $n \neq m$.

ε_n is the "spin-orbit free" vertical transition energy of state n.

Section S2.

The **W** matrix used in this work reads as follows, where the star stands for the conjugate transpose:

$$\mathbf{W} = \begin{pmatrix} \mathbf{W}^{\mathrm{T1,T1}} & \mathbf{W}^{\mathrm{T1,T2}} & \mathbf{W}^{\mathrm{T1,S1}} & \mathbf{W}^{\mathrm{T1,T3}} & \mathbf{W}^{\mathrm{T1,S2}} & \mathbf{W}^{\mathrm{T1,T4}} \\ \mathbf{W}^{*\mathrm{T1,T2}} & \mathbf{W}^{\mathrm{T2,T2}} & \mathbf{W}^{\mathrm{T2,S1}} & \mathbf{W}^{\mathrm{T2,T3}} & \mathbf{W}^{\mathrm{T2,S2}} & \mathbf{W}^{\mathrm{T2,T4}} \\ \mathbf{W}^{*\mathrm{T1,S1}} & \mathbf{W}^{*\mathrm{T2,S1}} & \mathbf{W}^{\mathrm{S1,S1}} & \mathbf{W}^{\mathrm{S1,T3}} & \mathbf{W}^{\mathrm{S1,S2}} & \mathbf{W}^{\mathrm{S1,T4}} \\ \mathbf{W}^{*\mathrm{T1,T3}} & \mathbf{W}^{*\mathrm{T2,T3}} & \mathbf{W}^{*\mathrm{S1,T3}} & \mathbf{W}^{\mathrm{T3,T3}} & \mathbf{W}^{\mathrm{T3,S2}} & \mathbf{W}^{\mathrm{T3,T4}} \\ \mathbf{W}^{*\mathrm{T1,S2}} & \mathbf{W}^{*\mathrm{T2,S2}} & \mathbf{W}^{*\mathrm{S1,S2}} & \mathbf{W}^{*\mathrm{T3,S2}} & \mathbf{W}^{\mathrm{S2,S2}} & \mathbf{W}^{\mathrm{S2,T4}} \\ \mathbf{W}^{*\mathrm{T1,T4}} & \mathbf{W}^{*\mathrm{T2,T4}} & \mathbf{W}^{*\mathrm{S1,T4}} & \mathbf{W}^{*\mathrm{T3,T4}} & \mathbf{W}^{*\mathrm{S2,T4}} & \mathbf{W}^{\mathrm{T4,T4}} \end{pmatrix}$$

Note that we explicitly consider the triplet's components, yielding a fourteen states **W** matrix. The different sub-matrices are defined as follows:

$$\mathbf{W}^{\mathrm{n,n}} = \varepsilon_n + \sum_{\mathrm{i} \in \mathrm{a}'} \kappa_i^{(n)} Q_i$$

$$\mathbf{W}^{\mathrm{S1,S2}} = \sum_{\mathrm{j} \in \mathrm{a}''} \lambda_j^{(\mathrm{S1,S2})} Q_j$$

$$\mathbf{W}^{\mathrm{Sn(A}'\mathrm{),Tm(A}'\mathrm{)}} = \mathbf{W}^{\mathrm{Sn(A''),Tm(A'')}} = \left(0;\ \eta_{\mathrm{Sn,Tm}};0\right)$$

$$\mathbf{W}^{\mathrm{Tm(A}'\mathrm{),Sn(A}'\mathrm{)}} = \mathbf{W}^{\mathrm{Tm(A''),Sn(A'')}} = \begin{pmatrix} 0 \\ \eta_{\mathrm{Sn,Tm}} \\ 0 \end{pmatrix}$$

$$\mathbf{W}^{\mathrm{Sn(A}'\mathrm{),Tm(A'')}} = \mathbf{W}^{\mathrm{Sn(A''),Tm(A}'\mathrm{)}} = \left(\eta^*_{\mathrm{Sn,Tm}};\ 0;\ \eta_{\mathrm{Sn,Tm}}\right)$$

$$\mathbf{W}^{\mathrm{Tm(A}'\mathrm{),Sn(A'')}} = \mathbf{W}^{\mathrm{Tm(A''),Sn(A}'\mathrm{)}} = \begin{pmatrix} \eta^*_{\mathrm{Sn,Tm}} \\ 0 \\ \eta_{\mathrm{Sn,Tm}} \end{pmatrix}$$

$$\mathbf{W}^{\mathrm{Tn(A\prime),Tm(A")}} = \mathbf{W}^{\mathrm{Tn(A"),Tm(A\prime)}} = \begin{pmatrix} \sum_{\mathrm{j\in a"}} \lambda_j^{(\mathrm{Tn,Tm})} Q_j & \eta_{\mathrm{Tn,Tm}} & 0 \\ -\eta^*_{\mathrm{Tn,Tm}} & \sum_{\mathrm{j\in a"}} \lambda_j^{(\mathrm{Tn,Tm})} Q_j & \eta_{\mathrm{Tn,Tm}} \\ 0 & -\eta^*_{\mathrm{Tn,Tm}} & \sum_{\mathrm{j\in a"}} \lambda_j^{(\mathrm{Tn,Tm})} Q_j \end{pmatrix}$$

$$\mathbf{W}^{\mathrm{Tn(A"),Tm(A")}} = \mathbf{W}^{\mathrm{Tn(A\prime),Tm(A\prime)}}$$

$$= \begin{pmatrix} \sum_{\mathrm{i\in a\prime}} \lambda_i^{(\mathrm{Tn,Tm})} Q_i + \eta_{\mathrm{Tn,Tm}} & 0 & 0 \\ 0 & \sum_{\mathrm{i\in a\prime}} \lambda_i^{(\mathrm{Tn,Tm})} Q_i & 0 \\ 0 & 0 & \sum_{\mathrm{i\in a\prime}} \lambda_i^{(\mathrm{Tn,Tm})} Q_i + \eta^*_{\mathrm{Tn,Tm}} \end{pmatrix}$$

where the SOC $\eta_{\mathrm{n,m}}$ constants (complex-valued) are obtained from electronic structure calculations at FC. The latter are kept constant in the wavepacket propagations. Notice that, due to symmetry selection rules, only a’ modes will give non-zero $\kappa_i^{(n)}$ and interstate coupling $\lambda_i^{(n,m)}$ between state of the same spacial symmetry, while only a’’ mode will couple states of different special symmetries.

Section S3.

Number of basis functions for the primitive basis as well as for the time-dependent (SPF) basis used in the MCTDH calculation for the lowest 14 electronic states of $[Re(CO)_3(phen)(L)]^+$ using the 15-modes model Hamiltonian described in the Results section of the main text. The Q_i labels correspond to $[Re(CO)_3(phen)(im)]^+$ conformer A but apply for all the other simulations.

Modes	Primitive basis	SPF basis
(Q_9, Q_{22}, Q_{27})	(23, 19, 19)	(11,11,15,11,15,11,11,11,11,11,11,9,9,9)
(Q_8, Q_{24}, $Q^{eff}_{36\text{-}37}$)	(13, 13, 13)	(8, 8, 8, 8, 8, 8, 8, 8, 8, 8, 8, 7, 7, 7)
(Q_{38}, Q_{70}, Q_{81})	(17, 17, 17)	(8, 8, 11, 8, 11, 8, 8, 8, 8, 8, 8, 7, 7, 7)
(Q_{88}, Q_{91}, Q_{93})	(17, 17, 17)	(8, 8, 11, 8, 11, 8, 8, 8, 8, 8, 8, 7, 7, 7)
(Q_{18}, Q_{32}, Q_{77})	(21, 19, 19)	(9, 9, 9, 9, 9, 9, 9, 9, 9, 9, 9, 7, 7, 7)

<table>
<tr><td colspan="6">$Re(CO)_3(phen)(imi)^+$</td></tr>
<tr><td colspan="3">Conf A</td><td colspan="3">Conf B</td></tr>
<tr><td colspan="2">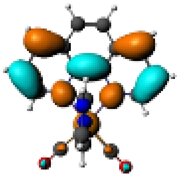</td><td>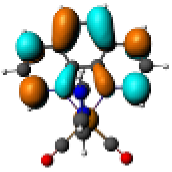</td><td colspan="2">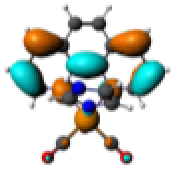</td><td>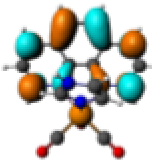</td></tr>
<tr><td colspan="2">79a’ -0.096</td><td>46a” -0.085</td><td colspan="2">124a -0.096</td><td>125a -0.086</td></tr>
<tr><td>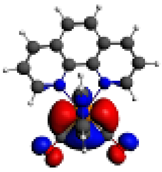</td><td>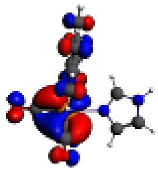</td><td>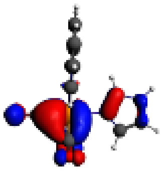</td><td>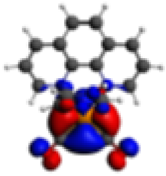</td><td>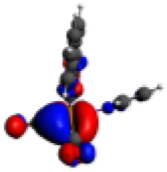</td><td>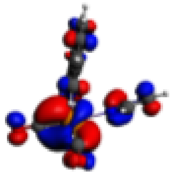</td></tr>
<tr><td>77a’ -0.252</td><td>78a’ -0.245</td><td>45a” -0.238</td><td>121a -0.252</td><td>122a -0.244</td><td>123a -0.240</td></tr>
<tr><td>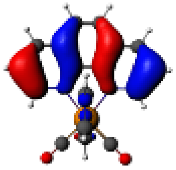</td><td>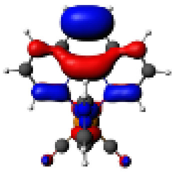</td><td>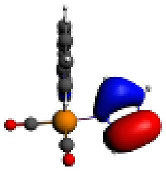</td><td>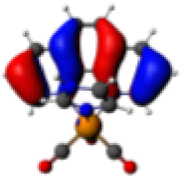</td><td>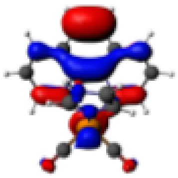</td><td>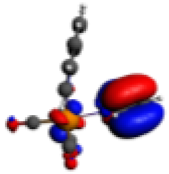</td></tr>
<tr><td>43a” -0.276</td><td>76a’ -0.266</td><td>44a” -0.258</td><td>118a -0.276</td><td>119a -0.266</td><td>120a -0.260</td></tr>
</table>

Figure S1. Kohn−Sham Frontier Orbitals of $Re(CO)_3(phen)(imi)^+$ conformer A (left) and B (right) in Water in the S_0 Electronic Ground State. Orbital energies are in a.u.

<table>
<tr><td colspan="12">Re(CO)$_3$(phen)(py)$^+$</td></tr>
<tr><td colspan="6">Conf A</td><td colspan="6">Conf B</td></tr>
<tr><td colspan="3">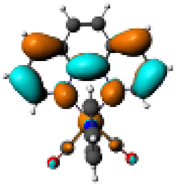</td><td colspan="3">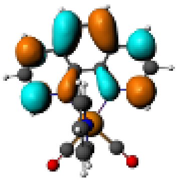</td><td colspan="3">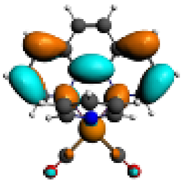</td><td colspan="3">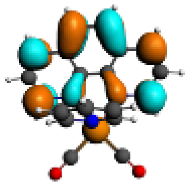</td></tr>
<tr><td colspan="3">82a’ -0.097</td><td colspan="3">46a” -0.085</td><td colspan="3">77a’ -0.097</td><td colspan="3">51a” -0.086</td></tr>
<tr><td colspan="2">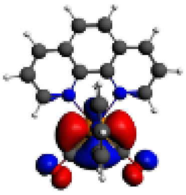</td><td colspan="2">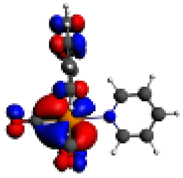</td><td colspan="2">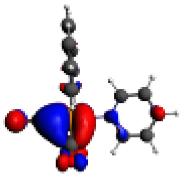</td><td colspan="2">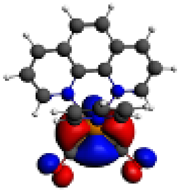</td><td colspan="2">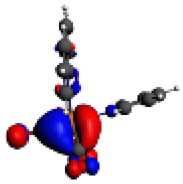</td><td colspan="2">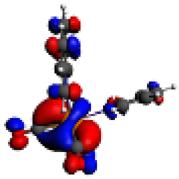</td></tr>
<tr><td colspan="2">80a’ -0.253</td><td colspan="2">81a’ -0.247</td><td colspan="2">45a” -0.242</td><td colspan="2">75a’ -0.255</td><td colspan="2">50a” -0.246</td><td colspan="2">76a’ -0.244</td></tr>
<tr><td colspan="2">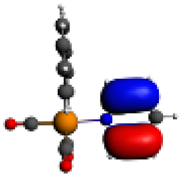</td><td colspan="2">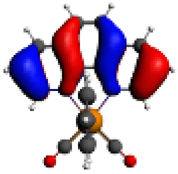</td><td colspan="2">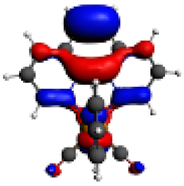</td><td colspan="2">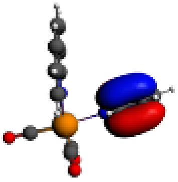</td><td colspan="2">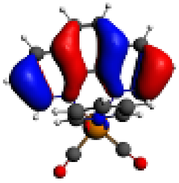</td><td colspan="2">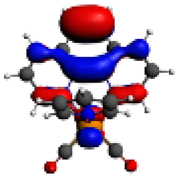</td></tr>
<tr><td colspan="2">43a” -0.285</td><td colspan="2">44a” -0.276</td><td colspan="2">79a’ -0.268</td><td colspan="2">48a” -0.286</td><td colspan="2">49a” -0.276</td><td colspan="2">74a’ -0.266</td></tr>
</table>

Figure S2. Kohn–Sham Frontier Orbitals of Re(CO)$_3$(phen)(py)$^+$ conformer A (left) and B (right) in Water in the S$_0$ Electronic Ground State. Orbital energies are in a.u.

Re(CO)$_3$(phen)(im)$^+$ conformer A

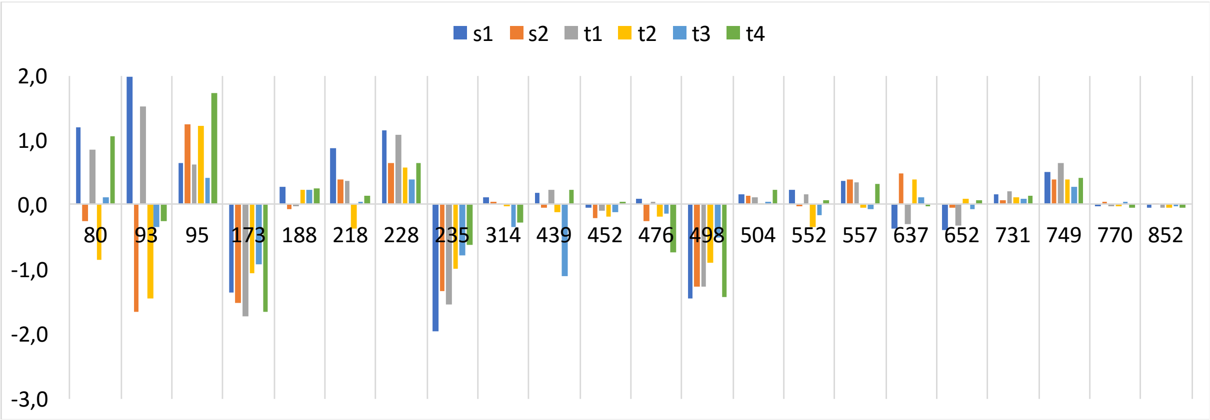

Re(CO)$_3$(phen)(py)$^+$ conformer A

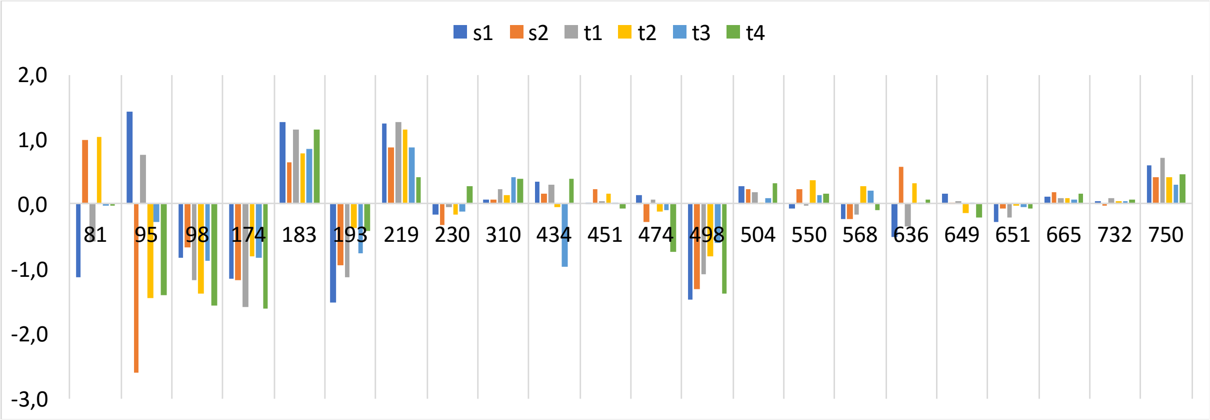

Re(CO)$_3$(phen)(py)$^+$ conformer B

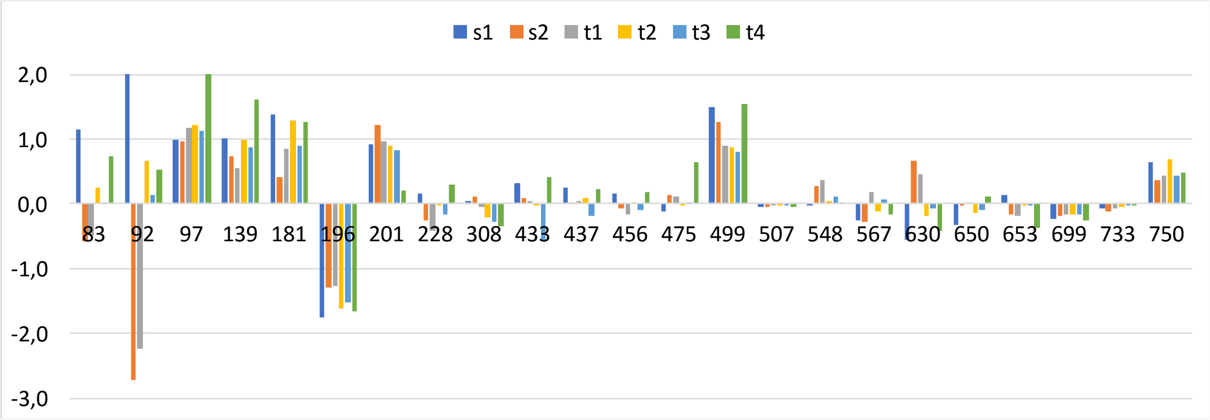

Figure S3. Displacement contributions of the a’ normal modes for each excited state considered herein of Re(CO)$_3$(phen)(im)$^+$ conformer A, and Re(CO)$_3$(phen)(py)$^+$ conformers A and B. Contribution of the modes between 80 - 850 cm^{-1}.

$Re(CO)_3(phen)(im)^+$ conformer A

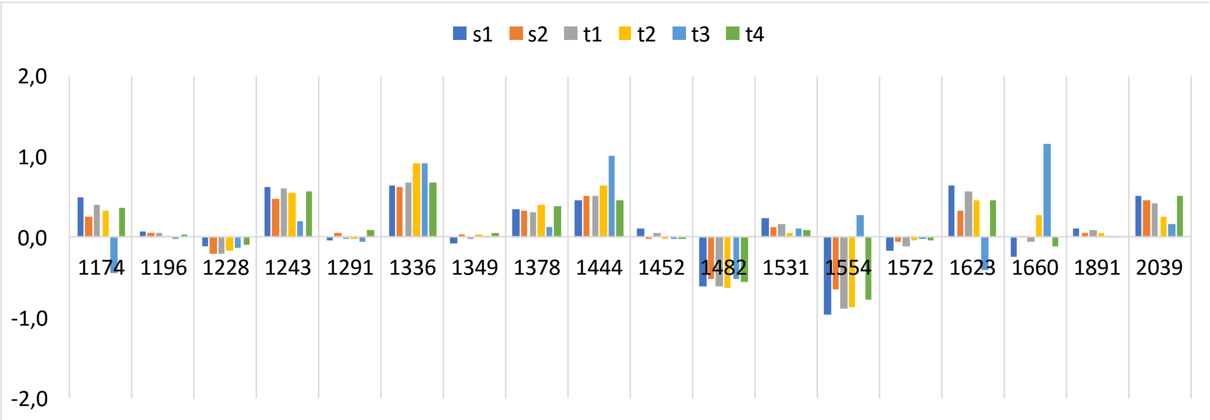

$Re(CO)_3(phen)(py)^+$ conformer A

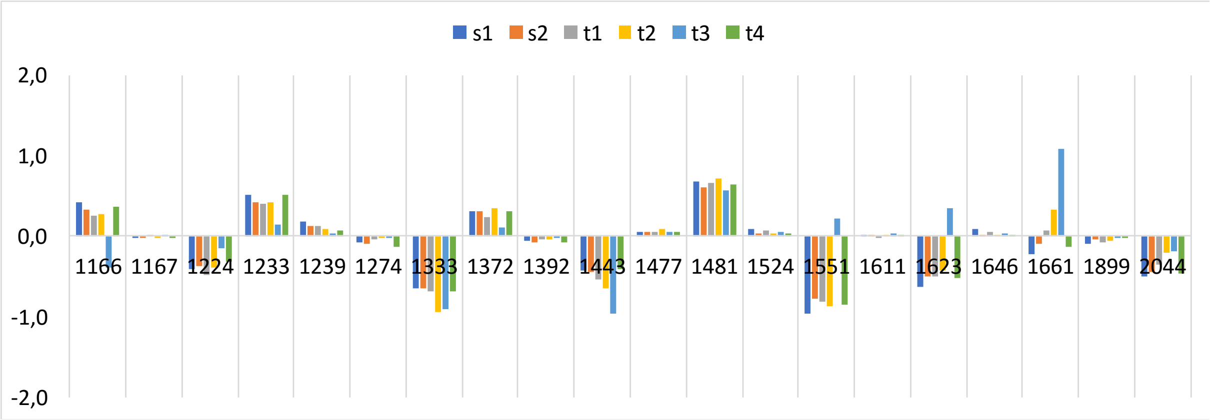

$Re(CO)_3(phen)(py)^+$ conformer B

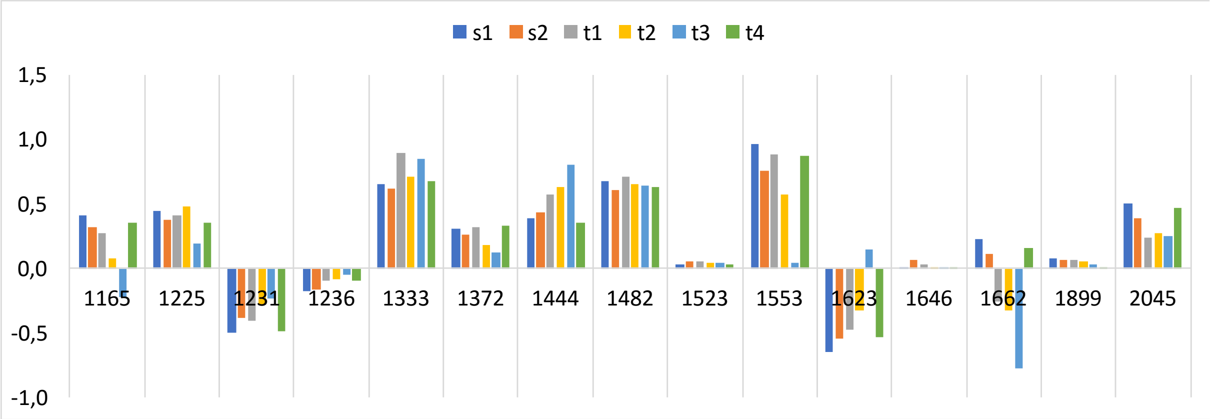

Figure S4. Displacement contributions of the a' normal modes for each excited state considered herein of $Re(CO)_3(phen)(im)^+$ conformer A, and $Re(CO)_3(phen)(py)^+$ conformers A and B. Contribution of the modes between 1165 - 2045 cm^{-1}.

Re(CO)$_3$(phen)(im)$^+$ conformer A

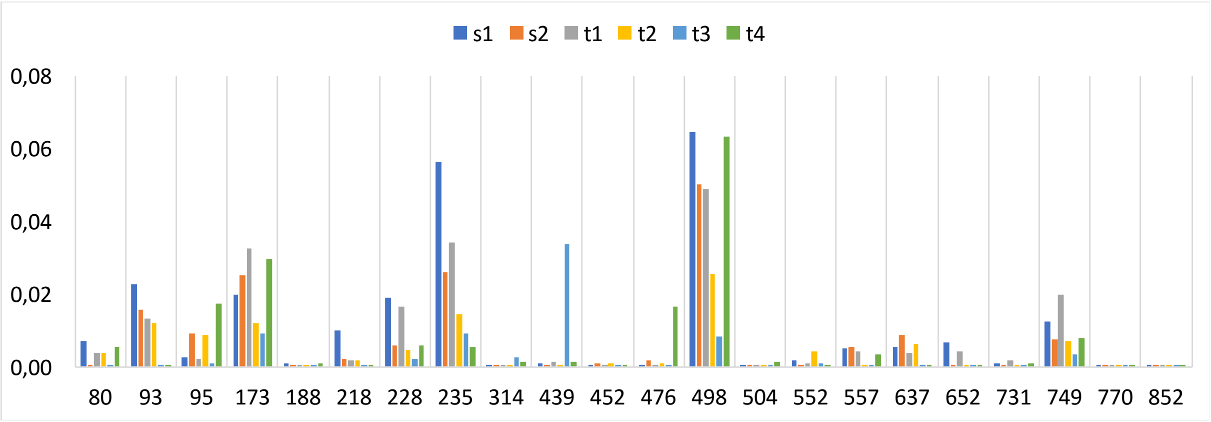

Re(CO)$_3$(phen)(py)$^+$ conformer A

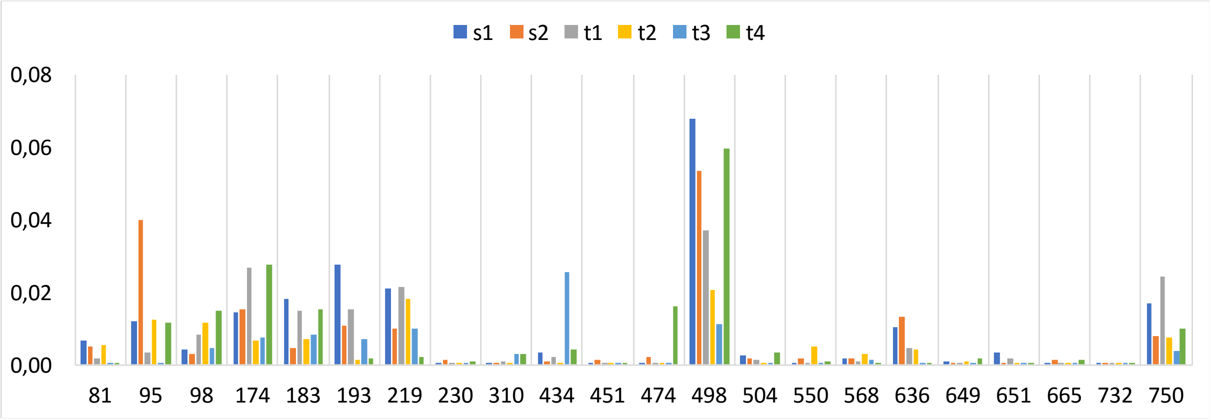

Re(CO)$_3$(phen)(py)$^+$ conformer B

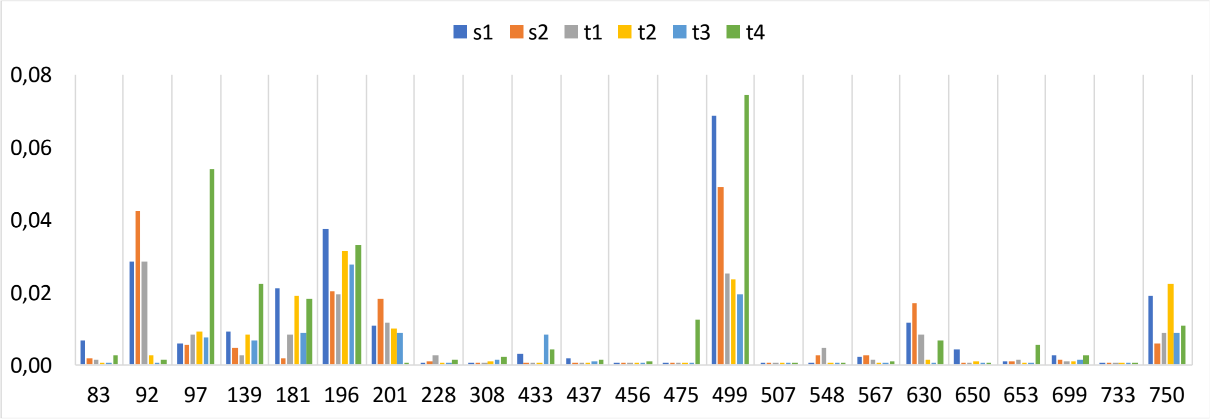

Figure S5. Energy-scaled contributions of the a’ normal modes for each excited state considered herein of Re(CO)$_3$(phen)(im)$^+$ conformer A, and Re(CO)$_3$(phen)(py)$^+$ conformers A and B. Contribution of the modes between 80 - 850 cm^{-1}.

$\mathrm{Re(CO)_3(phen)(im)^+}$ conformer A

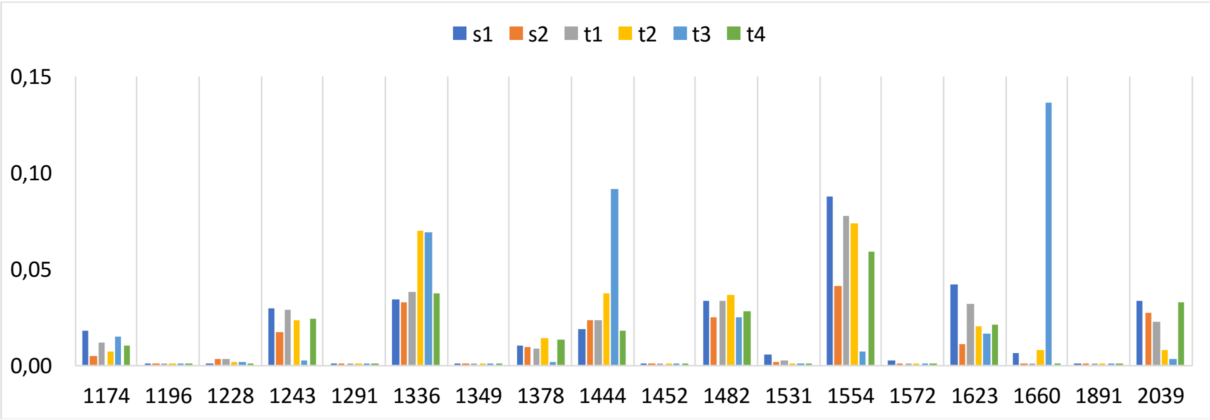

$\mathrm{Re(CO)_3(phen)(py)^+}$ conformer A

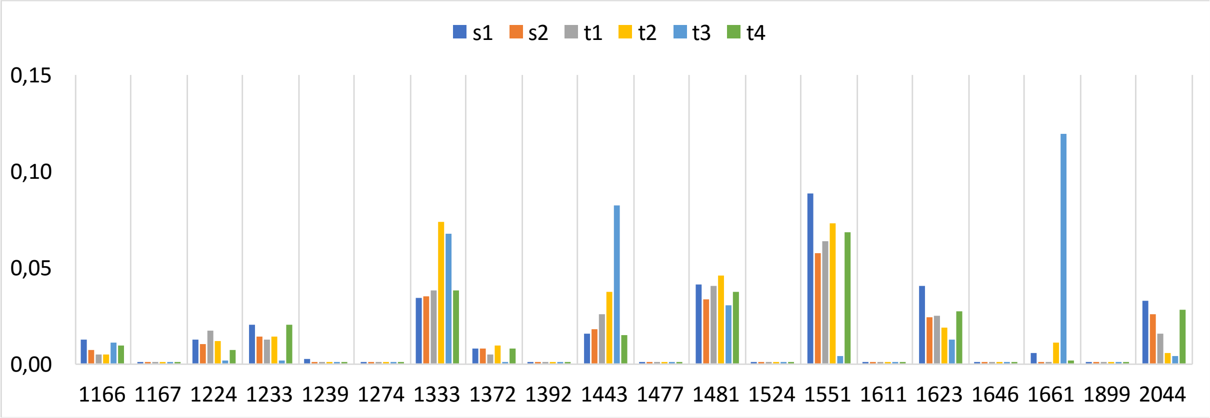

$\mathrm{Re(CO)_3(phen)(py)^+}$ conformer B

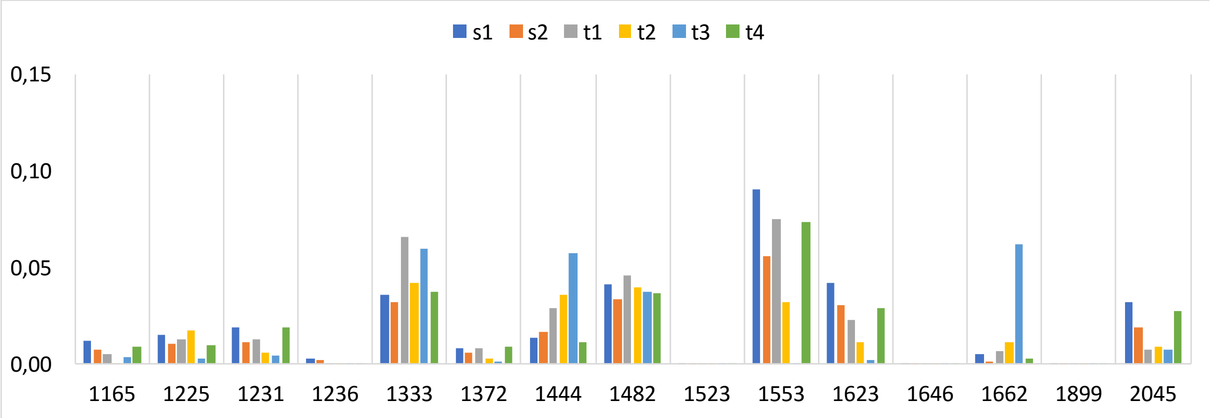

Figure S6. Energy-scaled contributions of the a’ normal modes for each excited state considered herein of $\mathrm{Re(CO)_3(phen)(im)^+}$ conformer A, and $\mathrm{Re(CO)_3(phen)(py)^+}$ conformers A and B. Contribution of the modes between 1165 - 2045 $\mathrm{cm^{-1}}$.

<table>
<tr><td>15-modes model</td><td>11-modes model</td></tr>
<tr><td colspan="2">[Re(CO)$_3$(phen)(im)]$^+$ conformer A</td></tr>
<tr><td>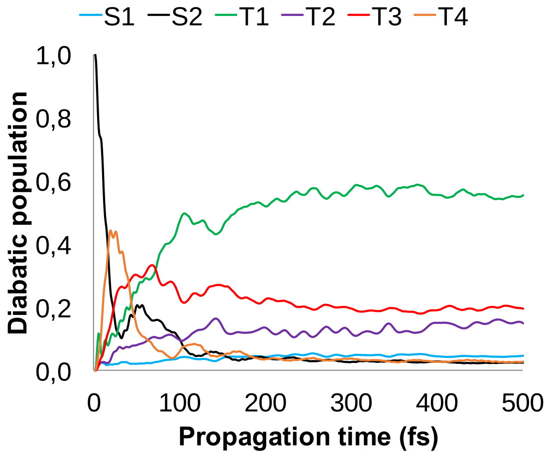 </td><td>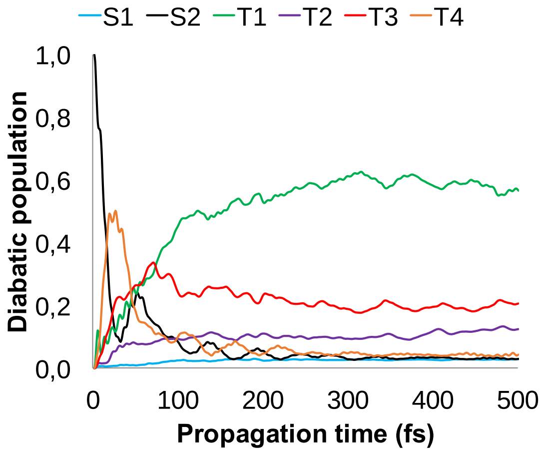 </td></tr>
</table>

Figure S7. Diabatic electronic populations of the six low-lying excited states of [Re(CO)$_3$(phen)(im)]$^+$ conformer A as a function of time including interstate coupling between same symmetry states when using the 15-modes model (left) and the 11-modes model (right) as described in the main text.

<table>
<tr><td>15-modes model</td><td>11-modes model</td></tr>
<tr><td colspan="2">[Re(CO)$_3$(phen)(py)]$^+$ conformer A</td></tr>
<tr><td>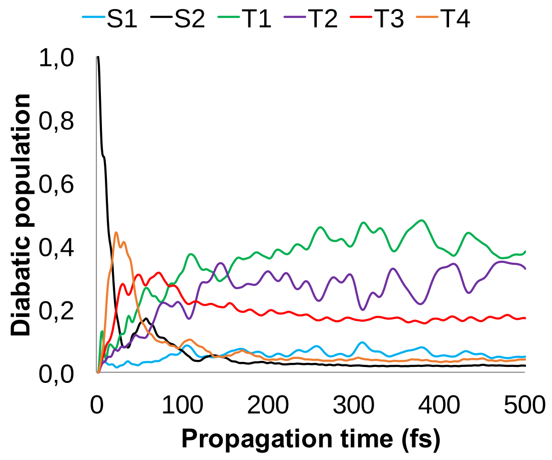
</td><td>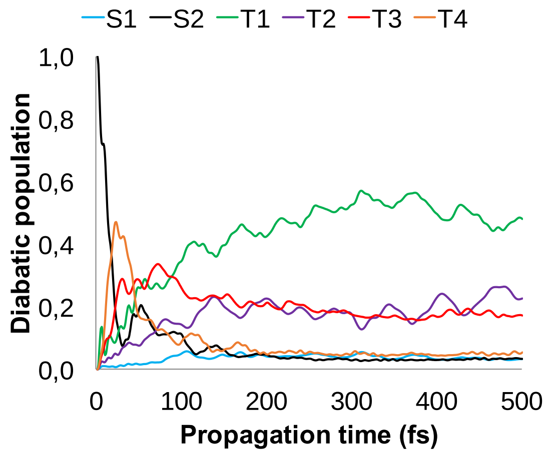
</td></tr>
<tr><td colspan="2">[Re(CO)$_3$(phen)(py)]$^+$ conformer B</td></tr>
<tr><td>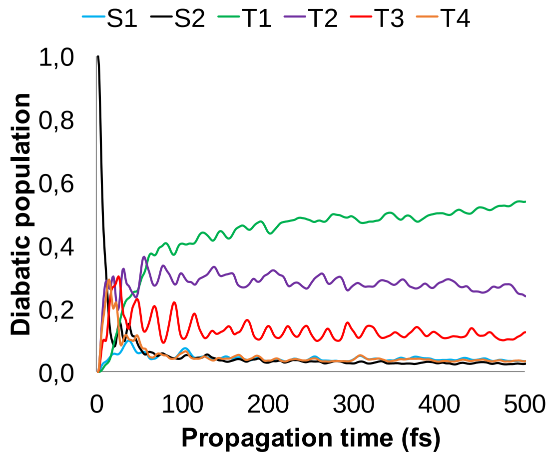
</td><td>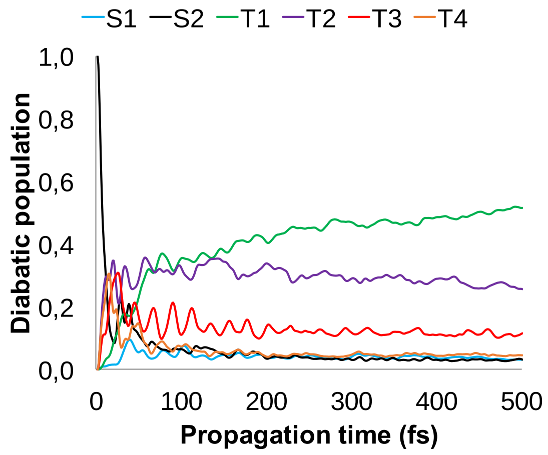
</td></tr>
</table>

Figure S8. Diabatic electronic populations of the six low-lying excited states of [Re(CO)$_3$(phen)(py)]$^+$ conformer A (top) and B (bottom) as a function of time including interstate coupling between same symmetry states when using the 15-modes model (left) and the 11-modes model (right) as described in the main text.

Table S1. TD-DFT/TDA transition energies (in eV), wavelengths of absorption (in nm) and oscillator strengths *f* associated to the low-lying excited states of Re(CO)$_3$(phen)(im)$^+$. The main one-electron excitations are indicated following the orbital notation depicted in Fig S1.

A conformer						**B conformer**					
State		One-electron excitation	Trans. E	Wave length	*f*	State		One-electron excitation	Trans. E	Wave length	*f*
T_1	A^3A''	83% 45a″-79a′	2.98	416		T_1	A^3A	87% 123-124	3.01	412	
T_2	A^3A'	84% 78a′-79a′	3.07	403		T_2	B^3A	57% 122-124 16% 123-125	3.05	406	
S_1	**a^1A''**	**99% 45a″-79a′**	**3.12**	**398**	**0.002**	T_3	C^3A	37% 123-125 34% 122-124 20% 119-125	3.25	382	
T_3	B^3A''	47% 78a′-46a″ 32% 76a′-46a″	3.24	382		**S_1**	**b^1A**	**56% 123-124** **41% 122-124**	**3.27**	**380**	**0.032**
S_2	**b^1A'**	**66% 78a′-79a′** **22% 45a″-46a″** **11% 77a′-79a′**	**3.40**	**365**	**0.054**	**S_2**	**c^1A**	**56% 122-124** **38% 123-124**	**3.33**	**373**	**0.075**
T_4	B^3A'	82% 77a′-79a′	3.42	363		T_4	D^3A	75% 121-124 15% 119-124	3.43	362	
T_5	C^3A'	82% 45a″-46a″	3.45	359		T_5	E^3A	38% 119-124 27% 122-125 20% 121-124	3.50	357	
S_3	c^1A'	80% 77a′-79a′	3.46	358	0.003	S_3	d^1A	97% 121-124	3.48	357	0.000
T_6	C^3A''	73% 43a″-79a′	3.56	348		T_6	F^3A	48% 122-125 32% 119-124	3.59	345	
S_4	d^1A'	59% 45a″-46a″ 30% 78a′-79a′	3.56	349	0.117	S_4	e^1A	91% 123-125	3.61	344	0.031
T_7	D^3A'	84% 76a′-79a′	3.57	347		T_7	G^3A	72% 118-124	3.61	343	
S_5	b^1A''	86% 78a′-46a″	3.76	329	0.024	S_5	f^1A	87% 122-125	3.67	338	0.046
T_8	D^3A''	27% 78a′-46a″ 28% 76a′-46a″ 33% 77a′-46a″	3.82	325		T_8	H^3A	41% 119-125 28% 123-125	3.73	332	
S_6	c^1A''	98% 44a″-79a′	3.83	324	0.002	T_9	I^3A	85% 120-124	3.81	325	
T_9	E^3A''	71% 44a″-79a′ 16% 43a″-79a′	3.84	323		S_6	g^1A	95% 120-124	3.83	324	0.019
T_{10}	E^3A'	67% 43a″-46a″	3.90	320		T_{10}	J^3A	82% 121-125	3.87	320	
S_7	d^1A''	95% 77a′-46a″	3.87	320	0.003	T_{11}	K^3A	83% 118-125	3.91	317	
S_8	e^1A'	77% 76a′-79a′	4.02	308	0.000	S_7	h^1A	99% 121-125	3.86	321	0.001
S_9	f^1A'	90% 44a″-46a″	4.19	296	0.011	S_8	i^1A	79% 119-124	4.03	307	0.003
S_{10}	e^1A''	42% 43a″-79a′ 53% 76a′-46a″	4.28	289	0.003	T_{12}	L^3A	73% 122-127 14% 123-127	4.01	313	

Table S2. TD-DFT/TDA transition energies (in eV), wavelengths of absorption (in nm) and oscillator strengths *f* associated to the low-lying excited states of $\mathrm{Re(CO)_3(phen)(py)^+}$. The main one-electron excitations are indicated following the orbital notation depicted in Fig S2.

A conformer						**B conformer**					
State		One-electron excitation	Trans. E	Wave length	*f*	State		One-electron excitation	Trans. E	Wave length	*f*
T_1	A^3A''	75% 45a"-82a'	3.03	409		T_1	A^3A'	86% 76a'-77a'	3.06	406	
T_2	A^3A'	84% 81a'-82a'	3.07	403		T_2	A^3A''	56% 50a"-77a' 19% 76a'-51a" 15% 74a'-51a"	3.07	403	
S_1	a^1A''	99% 45a"-82a'	3.21	386	0.002	T_3	B^3A''	37% 76a'-51a" 36% 50a"-77a' 24% 74a'-51a"	3.28	378	
T_3	B^3A''	46% 81a'-46a" 27% 79a'-46a" 20% 45a"-82a'	3.27	379		S_1	a^1A''	98% 50a"-77a'	3.32	373	0.001
T_4	B^3A'	88% 80a'-82a'	3.42	362		**S_2**	**b^1A'**	**90% 76a'-77a'**	**3.39**	**366**	**0.112**
S_2	**b^1A'**	**68% 81a'-82a'** **22% 80a'-82a'**	**3.43**	**362**	**0.067**	T_4	B^3A'	91% 75a'-77a'	3.49	356	
S_3	c^1A'	74% 80a'-82a' 14% 81a'-82a'	3.49	355	0.025	T_5	C^3A'	72% 74a'-77a'	3.51	353	
T_5	C^3A'	79% 45a"-46a"	3.55	350		S_3	c^1A'	97% 75a'-77a'	3.52	352	0.006
T_6	C^3A''	89% 44a"-82a'	3.58	346		T_6	C^3A''	86% 49a"-77a'	3.61	343	
T_7	D^3A'	74% 79a'-82a' 15% 45a"-46a"	3.60	344		T_7	D^3A'	82% 50a"-51a" 11% 74a'-77a'	3.63	342	
S_4	d^1A'	79% 45a"-46a" 15% 81a'-82a'	3.66	339	0.097	S_4	d^1A'	87% 50a"-51a"	3.72	333	0.067
T_8	E^3A'	80% 45a"-47a"	3.74	331		S_5	b^1A''	90% 76a'-51a"	3.72	333	0.025
S_5	b^1A''	84% 81a'-46a"	3.81	325	0.023	T_8	D^3A''	55% 74a'-51a" 40% 76a'-51a"	3.81	325	
T_9	D^3A''	49% 80a'-46a" 28% 81a'-46a" 21% 79a'-46a"	3.85	322		T_9	E^3A'	84% 49a"-51a"	3.91	317	
T_{10}	F^3A'	88% 44a"-46a"	3.91	317		T_{10}	E^3A''	99% 75a'-51a"	3.92	316	
S_6	c^1A''	93% 80a'-46a"	3.92	317	0.004	S_6	c^1A''	99% 75a'-51a"	3.93	316	0.000
T_{11}	E^3A''	47% 80a'-46a" 40% 79a'-46a"	3.95	314		T_{11}	F^3A'	73% 76a'-78a'	3.97	312	
T_{12}	F^3A''	34% 80a'-47a" 26% 81a'-47a" 20% 80a'-48a"	4.02	309		S_7	e^1A'	80% 74a'-77a'	4.03	308	0.004
S_7	e^1A'	84% 79a'-82a'	4.04	307	0.000	T_{12}	G^3A'	83% 50a"-52a"	4.03	308	
T_{13}	G^3A''	46% 81a'-47a" 14% 80a'-47a"	4.07	305		T_{13}	F^3A''	45% 75a'-52a" 39% 76a'-52a"	4.11	302	

Table S3. TD-DFT/TDA transition energies (in eV), wavelengths of absorption (in nm), oscillator strengths *f* associated to the low-lying "spin-orbit" states E$_i$ of Re(CO)$_3$(phen)(im)$^+$ (top) and Re(CO)$_3$(phen)(py)$^+$ (bottom) conformer A and B in water. The composition of each state is given as function of the singlet and triplet components reported in Tables S1 and S2.

	Re(CO)$_3$(phen)(im)$^+$									
	A conformer					B conformer				
	State	Composition	Trans. E (eV)	Wave length (nm)	*f*	State	Composition	Trans. E (eV)	Wave length (nm)	*f*
E1	A''	T1 75% T2 18%	2.91	426	0.000	A	T1 60% T2 28%	2.94	421	0.000
E2	A'	T1 75% T2 18%	2.92	425	0.001	A	T1 60% T2 30%	2.95	421	0.000
E3	A'	T1 90%	2.94	422	0.003	A	T1 85%	2.97	417	0.005
E4	A''	T2 48% S1 42%	2.99	415	0.001	A	T2 83%	3.01	412	0.005
E5	A''	T2 75% T1 20%	3.09	401	0.000	A	T2 64% T1 21%	3.08	403	0.000
E6	A'	T2 75% T1 20%	3.09	401	0.000	A	T2 65% T1 30%	3.08	403	0.000
E7	A''	S1 48% T2 50%	3.15	394	0.001	**A**	T3 65% S1 12%	3.20	388	0.008
E8	A'	T3 90%	3.22	385	0.004	A	T3 82%	3.24	383	0.000
E9	A''	T3 88%	3.24	383	0.000	A	T3 84%	3.24	383	0.000
E10	A'	T3 88%	3.24	383	0.000	**A**	**S1 47% S2 12%**	**3.25**	**382**	**0.024**
E11	**A'**	**S2 59% T4 19%**	**3.37**	**368**	**0.033**	**A**	**S2 52% T3 20%**	**3.33**	**372**	**0.043**
E12	A''	T5 60% T4 24%	3.39	366	0.001	A	T4 60% T5 22%	3.42	363	0.000
E13	A''	T5 56% T4 30%	3.39	365	0.001	A	T4 42% S3 16%	3.42	362	0.001
E14	A'	T5 56% T4 19%	3.40	365	0.003	**A**	T5 28% T4 21%	3.44	361	0.010

	Re(CO)$_3$(phen)(py)$^+$									
	A conformer					B conformer				
	State	Composition	Trans. E (eV)	Wave length (nm)	*f*	State	Composition	Trans. E (eV)	Wave length (nm)	*f*
E1	A''	T1 65% T2 26%	2.96	419	0.000	A''	T1 52% T2 38%	2.98	416	0.000
E2	A'	T1 65% T2 27%	2.96	419	0.002	A'	T1 54% T2 38%	2.98	416	0.000
E3	A'	T1 89%	2.99	415	0.003	A''	T1 86%	3.02	411	0.000
E4	A''	T2 70% S1 22%	3.02	411	0.000	A'	T2 88%	3.04	408	0.007
E5	A''	T2 66% T1 29%	3.10	400	0.000	A''	T2 58% T1 38%	3.10	400	0.000
E6	A'	T2 67% T1 30%	3.10	400	0.000	A'	T2 58% T1 38%	3.10	400	0.000
E7	A''	S1 59% T2 28%	3.20	388	0.001	A'	T3 74% S2 10%	3.24	383	0.011
E8	A'	T3 85%	3.24	382	0.003	A''	T3 84%	3.27	379	0.000
E9	A''	T3 86%	3.26	381	0.000	A'	T3 85%	3.27	379	0.000
E10	A'	T3 88%	3.26	380	0.001	A''	S1 60% T4 15%	3.28	379	0.001
E11	**A'**	**S2 34% T4 33%**	**3.40**	**364**	**0.025**	**A'**	**S2 61% T3 18%**	**3.39**	**365**	**0.069**
E12	A''	T4 66% T5 12%	3.43	361	0.000	A''	T5 40% T4 40%	3.46	359	0.000
E13	A'	S2 31% T5 19%	3.45	360	0.025	A'	T5 44% S3 22%	3.47	358	0.002
E14	A''	T4 64% T5 15%	3.46	358	0.001	A''	T5 40% S1 17%	3.50	354	0.003

Table S4. Intrastate coupling values $\kappa^{(n)}$ (in eV) associated with each excited state n, and interstate coupling values $\lambda^{(n,m)}$ (in eV) between same symmetry states (top) and different symmetry states (bottom), determined for the selected a’ and a” normal modes, respectively $Re(CO)_3(phen)(im)^+$ conformer A. The frequencies ω (in cm^{-1}) are indicated.

a'	S1	S2	T1	T2	T3	T4	T1/T3	T2/T4
93	0.0228	-0.0190	0.0174	-0.0166	-0.0041	-0.0029	0.0000	0.0076
235	-0.0573	-0.0388	-0.0447	-0.0289	-0.0229	-0.0179	0.0095	0.0000
439	0.0095	-0.0023	0.0123	-0.0062	-0.0608	0.0119	0.0189	0.0000
498	-0.0892	-0.0786	-0.0777	-0.0562	-0.0317	-0.0883	0.0138	0.0226
552	0.0149	-0.0019	0.0111	-0.0244	-0.0112	0.0049	0.0185	0.0205
637	-0.0297	0.0375	-0.0239	0.0315	0.0089	-0.0019	0.0189	0.0000
1174	0.0723	0.0379	0.0593	0.0469	-0.0652	0.0539	0.0414	0.0000
1336	0.1065	0.1044	0.1119	0.1517	0.1510	0.1116	0.0000	0.0000
1444	0.0827	0.0921	0.0919	0.1161	0.1806	0.0809	0.0373	0.0189
1554	-0.01838	-0.1254	-0.1726	-0.1687	0.0539	-0.1510	0.0462	0.0000
1623	0.1294	0.0673	0.1139	0.0907	-0.0808	0.0917	0.0481	0.0000
1660	-0.0499	0.0016	-0.0110	0.0572	0.2367	-0.0224	0.0821	0.0000

a"	S1/S2	T1/T2	T2/T3	T3/T4
90	0.0158	0.0061	0.0000	0.0129
475	0.0195	0.0378	0.0000	0.0057
626*	0.0393	0.0226	0.0000	0.0349

Table S5. Intrastate coupling values $\kappa^{(n)}$ (in eV) associated with each excited state *n*, and interstate coupling values $\lambda^{(n,m)}$ (in eV) between same symmetry states (top) and different symmetry states (bottom), determined for the selected a' and a" normal modes of $Re(CO)_3(phen)(py)^+$ conformer A, respectively. The frequencies ω (in cm^{-1}) are indicated.

a'	S1	S2	T1	T2	T3	T4	T1/T3	T2/T4
95	-0.0169	0.0306	-0.0090	0.0170	0.0032	0.0166	0.0040	0.0000
219	-0.0336	-0.0234	-0.0342	-0.0314	-0.0234	-0.0113	0.0000	0.0205
434	-0.0191	-0.0092	-0.0158	0.0027	0.0524	-0.0216	0.0332	0.0130
498	0.0913	0.0811	0.0675	0.0503	0.0375	0.0858	0.0220	0.0239
550	0.0040	-0.0161	0.0014	-0.0257	-0.0095	-0.0112	0.0162	0.0210
636	0.0407	-0.0455	0.0267	-0.0256	-0.0003	-0.0061	0.0213	0.0000
1166	-0.0605	-0.0463	-0.0373	-0.0382	0.0575	-0.0524	0.0480	0.0000
1333	0.1068	0.1070	0.1120	0.1556	0.1490	0.1127	0.0000	0.0000
1443	0.0758	0.0811	0.0956	0.1152	0.1715	0.0727	0.0467	0.0307
1551	0.1843	0.1490	0.1565	0.1677	-0.0413	0.1621	0.0805	0.0219
1623	0.1271	0.0991	0.1002	0.0877	-0.0713	0.1052	0.0821	0.0261
1661	0.0466	0.0202	-0.0145	-0.0665	-0.2218	0.0285	0.1143	0.0352

a"	S1/S2	T1/T2	T2/T3	T3/T4
90	0.0177	0.0038	0.0000	0.0016
476	0.0221	0.0354	0.0000	0.0100
627*	0.0447	0.0191	0.0000	0.0338

Table S6. Intrastate coupling values $\kappa^{(n)}$ (in eV) associated with each excited state *n*, and interstate coupling values $\lambda^{(n,m)}$ (in eV) between same symmetry states (top) and different symmetry states (bottom), determined for the selected a' and a" normal modes of $Re(CO)_3(phen)(py)^+$ conformer B, respectively. The frequencies ω (in cm^{-1}) are indicated.

a'	S1	S2	T1	T2	T3	T4	T2/T3	T1/T4
92	-0.0254	0.0311	0.0254	-0.0076	-0.0016	-0.0059	0.0108	0.0000
201	-0.0231	-0.0301	-0.0239	-0.0224	-0.0209	-0.0052	0.0000	0.0187
433	-0.0175	-0.0044	-0.0018	0.0015	0.0298	-0.0218	0.0224	0.0000
499	-0.0921	-0.0777	-0.0559	-0.0540	-0.0492	-0.0959	0.0360	0.0000
548	0.0010	0.0190	-0.0253	-0.0037	-0.0078	-0.0021	0.0000	0.0205
630	0.0425	-0.0517	-0.0365	0.0153	0.0054	0.0326	0.0141	0.0000
1165	-0.0589	-0.0455	-0.0386	-0.0112	0.0324	-0.0515	0.0098	0.0000
1333	-0.1081	-0.1025	-0.1474	-0.1173	-0.1400	-0.1114	0.0249	0.0239
1444	-0.0696	-0.0771	-0.1015	-0.1125	-0.1434	-0.0625	0.0184	0.0000
1553	-0.1861	-0.1461	-0.1695	-0.1107	-0.0084	-0.1679	0.0513	0.0000
1623	0.1299	0.1104	0.0954	0.0660	-0.0282	0.1079	0.0512	0.0373
1662	-0.0472	-0.0228	0.0521	0.0682	0.1596	-0.0326	0.0102	0.0344

a"	S1/S2	T1/T2	T1/T3	T3/T4
93	0.0136	0.0068	0.0000	0.0209
474	0.0205	0.0301	0.0821	0.0075
627*	0.0296	0.0000	0.0000	0.0429